Temperature and Doping-Dependent Renormalization Effects of the Low Energy Electronic Structure of $Ba_{1-x}K_xFe_2As_2$ Single Crystals

A. Koitzsch,[1] D. S. Inosov,[1,2] D. V. Evtushinsky,[1] V. B. Zabolotnyy,[1] A. A. Kordyuk,[1,3] A. Kondrat,[1] C. Hess,[1] M. Knupfer,[1] B. Büchner,[1] G. L. Sun,[2] V. Hinkov,[2] C. T. Lin,[2] A. Varykhalov,[4] and S. V. Borisenko[1]

[1]*Institute for Solid State Research, IFW-Dresden, P.O.Box 270116, D-01171 Dresden, Germany*
[2]*Max-Planck-Institute for Solid State Research, Heisenbergstraße 1, D-70569 Stuttgart, Germany*
[3]*Institute of Metal Physics of National Academy of Sciences of Ukraine, 03142 Kyiv, Ukraine*
[4]*BESSY GmbH, Albert-Einstein-Strasse 15, 12489 Berlin, Germany*

(Received 3 November 2008; revised manuscript received 30 January 2009; published 21 April 2009)

We investigate the low energy electronic structure of $Ba_{1-x}K_xFe_2As_2$ ($x = 0$; 0.3, $T_c = 32$ K) single crystals by angle-resolved photoemission spectroscopy with a focus on the renormalization of the dispersion. A kink feature is detected at $E \approx 25$ meV for the doped compound which vanishes at $T = 200$ K but stays virtually constant when T_c is crossed. Our experimental findings rule out the magnetic resonance mode as the origin of the kink and render conventional electron-phonon coupling unlikely. They put stringent restrictions on the dominant source of the electronic interaction channel.

DOI: 10.1103/PhysRevLett.102.167001 PACS numbers: 74.25.Jb, 74.20.Mn, 74.62.Dh, 79.60.−i

The discovery of superconductivity in FeAs-based pnictides with transition temperatures up to $T_c = 56$ K has received widespread attention in the solid state physics community [1,2]. One of the most important questions posed by the new materials concerns the nature of the electron pairing interaction. While conventional superconductivity is mediated by phonons, the pairing mechanism for the pnictides is unclear. The symmetry of the order parameter is *s*-wave-like [3–7], but calculations indicate that conventional electron-phonon interaction is too weak to account for the high transition temperatures [8]. Another type of bosonic excitations that could mediate the pairing are spin fluctuations. The parent compounds of the pnictides show phase transitions around $T \approx 140$ K [9,10] to an orthorhombic structure and a spin-density wave state (SDW). The phase transitions are suppressed by doping but spin fluctuations may still be present. A magnetic resonance mode has been observed below T_c [11] and an extended *s*-wave order parameter has been proposed to account for this observation [12].

A direct fingerprint of the electron-interaction channel is represented by the renormalization of the band structure near the Fermi energy (E_F). The latter affects a large number of low energy properties of the solid, such as its resistivity, but can be monitored best by angle-resolved photoemission (ARPES). The so called ''kink'' features have been widely discussed for the cuprates [13] and are already reported for the iron arsenide's as well [14,15]. Here we perform a temperature and doping-dependent ARPES study of the ''kinks'' in the $Ba_{1-x}K_xFe_2As_2$ system ($x = 0$; 0.3, $T_c = 32$ K). We determine their characteristic properties and shed light on the nature of the underlying boson. Additionally, we measured the resistance of the doped sample and find similarities between the low energy renormalization seen by ARPES and macroscopic transport properties.

ARPES data were collected from the cleaved surface of high quality single crystals using synchrotron radiation (''1^3-ARPES'' at BESSY) within the range of photon energies 50–80 eV. The component of the electric field vector of the incoming light parallel to the sample surface was perpendicular to the analyzer slit except stated otherwise. The overall energy and momentum resolutions were set to ~2 meV and to ~0.013 $Å^{-1}$, respectively, for the low temperature measurements.

The single crystals of $Ba_{1-x}K_xFe_2As_2$ ($x = 0$, 0.3) were grown using Sn flux in a ZrO_2 crucible by a specially designed apparatus. The free-standing as-grown crystals can be readily separated by decanting the residual flux. The growth details are described in Ref. [16]. Resistance was measured by a standard four probe technique by alternating dc current.

We start with the presentation of the results for $Ba_{0.7}K_{0.3}Fe_2As_2$. Figure 1(a) shows a piece of the measured Fermi surface reproduced from [17] to illustrate the momentum space locations under scrutiny here. The Fermi surface as seen in ARPES consists of two nearly concentric hole-like barrels around the Γ point and a cross-like feature at the zone corner, which itself is built by four hole pockets symmetric to the X point and a small electron pocket directly at the X point. We focus on the high symmetry directions ΓM and ΓX. To this end high resolution photoemission spectra have been recorded along the blue bars as a function of energy and temperature. Examples of such measurements are shown in Figs. 1(b) and 1(c) for $T = 10$ K. By choosing appropriate photon energy and polarization conditions and depending on the measuring direction, the intensity of the relevant bands can be enhanced or diminished. This is particularly obvious when comparing Figs. 1(b) and 1(c). In the former case ($h\nu = 50$ eV) both hole-like bands surrounding the Γ-point are clearly visible. However, the intensity of the outer hole-like band is

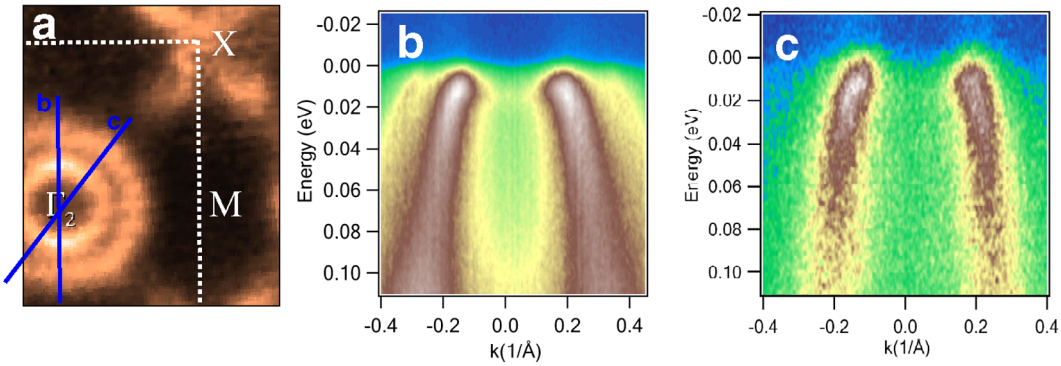

FIG. 1 (color online). Low energy electronic structure of $Ba_{0.7}K_{0.3}Fe_2As_2$. (a) Fermi surface with Brillouin zone boundary (white dotted line). The blue lines indicate positions of the energy dependent measurements shown in (b) and (c). A slight bending of the dispersion at low energies ($\approx$25 meV) is visible even in these false color representations.

completely suppressed in Fig. 1(c) ($h\nu = 80$ eV, parallel polarization). Closer inspection of Fig. 1(b) and 1(c) reveals already visually the existence of a bending of the dispersion, i.e., a kink feature, at low energies ($E \approx$ 20–40 meV), especially for Fig. 1(c). This observation will be substantiated below in the context of Figs. 2 and 3.

From data sets such as presented in Fig. 1 an abundance of information can be extracted. Here we focus on the dispersion of the bands which are obtained by fitting horizontal cuts of those data sets to Lorentzian line shapes. An example is presented in Fig. 2(b) for the intensity at $E = 49$ meV for Fig. 1(b). The data are fitted by four Lorentzians plus a linear background. The dispersion is derived from the peak positions. Figure 2(a) summarizes the dispersions along ΓM for a variety of temperatures for the left branches of the barrels. Let us focus first on the inner band. The first obvious observation is that the dispersion is nearly linear from $E = 110$ meV to $E \approx 40$ meV and then undergoes a reduction of the slope. This represents the famous kink feature, situated here at $E \approx$ 25 meV in agreement with previous studies [14,15]. Although less obvious and superimposed by a smooth curved dispersion we find also a kink for the outer band. The kink strength, i.e., the change of the slope, is smaller and the kink energy is possibly shifted to somewhat lower energy.

Now we turn to the temperature dependence of the inner Γ band. It is very clear from the data that there are only weak changes to the kink feature for $T \leq 100$ K. However, at $T = 150$ K the kink is substantially weaker, and the dispersion has completely straightened out at $T = 200$ K. This observation has far reaching consequences. It is in qualitative agreement with [15] where only weak changes are reported below $T < 40$ K, but different from the data interpretation in [14] where it is concluded that the kink vanishes crossing T_c. The kink at the Γ-barrel shown in Fig. 2 is obviously not associated with the onset of superconductivity at $T_c = 32$ K. It might be that additional small changes occur when T_c is crossed, a question we leave for future studies.

Figure 2(c) presents the dispersion for the ΓX direction, i.e., for the zone diagonal. The result is similar to the ΓM direction: a straight dispersion below $E = 40$ meV is followed by a kink at $E \approx 30$ meV. This shows that the kink energy does not vary substantially as a function of the direction.

We turn now to the undoped compound $BaFe_2As_2$. The Fermi surface [Fig. 3(a)] consists again of a hole pocket around Γ, though with a smaller volume due to the miss-

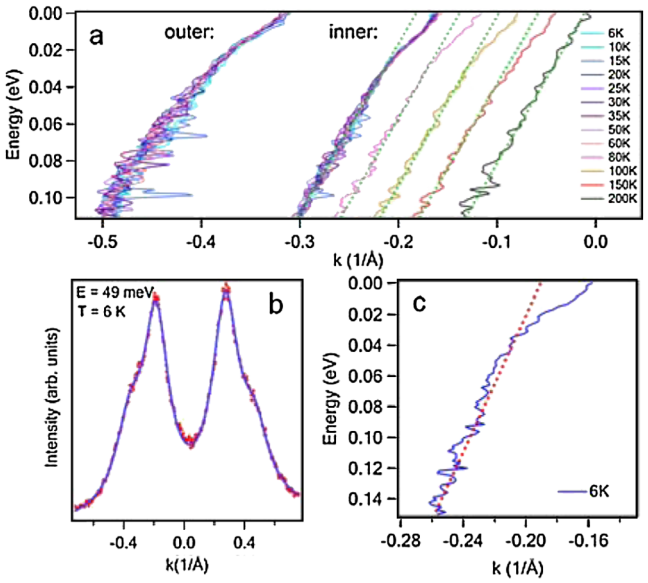

FIG. 2 (color online). (a) Dispersions for $Ba_{0.7}K_{0.3}Fe_2As_2$ as a function of temperature along ΓM. The two clusters of curves belong to the outer and inner Γ-barrels, respectively. The dispersions above 60 K are horizontally shifted for clarity. The green dotted lines are guides to the eye and parallel. (b) Example of a horizontal cut through the data in Fig. 1(b) and the fit with four Lorentzians plus linear background. (c) Dispersion along ΓX.

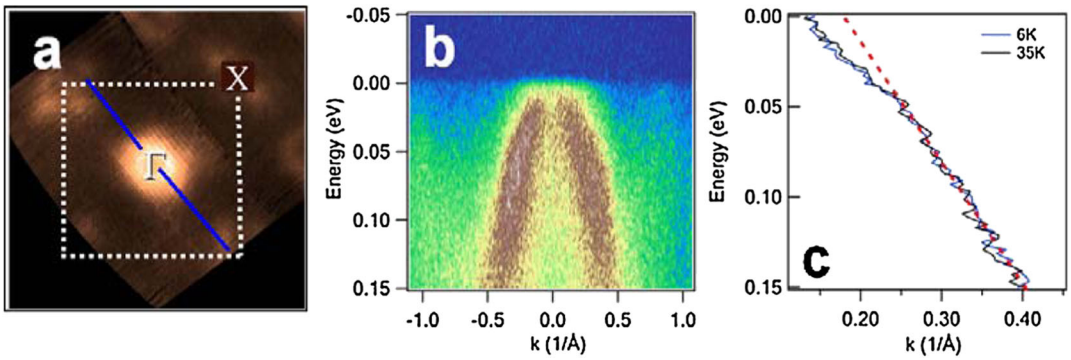

FIG. 3 (color online). Low energy electronic structure of undoped $BaFe_2As_2$. (a) Fermi surface map. The dotted lines reflect the Brillouin zone boundaries. (b) Energy dependence of the photoemission intensity along the blue line in (a). (c) Extracted dispersion for $T = 6$ K and 35 K. The red dashed line is a guide to the eye.

ing holes compared to the doped compound. The energy dependence along the blue line in Fig. 3(a) is shown in Fig. 3(b). Note that this cut is somewhat off the ΓX direction but sufficiently close to allow comparison to the ΓX direction of the doped compound. The extracted dispersion is presented in Fig. 3(c) for $T = 6$ K and 35 K. Applying the same approximate procedure as in Fig. 2 to visualize the kink, namely, extending the linear dispersion at higher energies to lower energies, clearly shows its existence. The energy position of the kink is $E \approx 45$ meV, i.e., somewhat larger than for the doped compound. Note that the rigorous way to determine the kink energy requires the self consistent analysis of the data within the self energy formalism [18].

Which interaction is the physical origin of the kink feature in $Ba_{1-x}K_xFe_2As_2$? The standard suspects are phonons and magnons in some form. The observed kink energy of $E = 25$–45 meV would be consistent with the observed phonon spectrum [19]. But important arguments against strong electron-phonon coupling as origin of the kink come from the temperature dependence and the observed coupling strength. A lower limit of the latter can be estimated from Fig. 2(a) by approximating the bare dispersion with the $T = 200$ K data. Extracting the real part of the self energy ($\Sigma'(E)$) for the low temperature data and exploiting $\lambda = -(d\Sigma'/dE)_{E=0}$ we obtain $\lambda \geq 0.5$, a value much larger than the prediction for conventional electron-phonon coupling $\lambda = 0.21$ [8]. The vanishing of the kink at ~200 K and its constancy below 100 K are difficult to reconcile with a purely phonon dominated self energy. These observations are supported by Raman studies [20–22] and neutron scattering [19]. However, other studies suggest that substantial electron-phonon coupling cannot be totally excluded [23–25].

Equivalent experimental data for the magnetic excitation spectrum are more difficult to obtain. So far the appearance of a magnetic resonance mode below T_c at $E = 13$ meV has been reported [11]. This feature cannot explain the kink of the undoped, nonsuperconducting parent compound, and its energy is too low. Also it misfits the observed temperature dependence of the doped compound because the kink hardly changes when T_c is crossed, whereas the resonance mode vanishes.

Having excluded standard electron-phonon coupling and the magnetic resonance mode as the source of the kink renormalization in the iron arsenides, we focus our attention on antiferromagnetic fluctuations. Undoped $BaFe_2As_2$ has a sharp, highly dispersive spin wave spectrum extending up to an energy of 170 meV [26]. The phase transitions that the parent compounds undergo lead to specific features, e.g., in the resistivity vs T dependence. Those features are still recognizable for the doped compounds where the magnetic order has vanished. This indicates that fluctuations connected with the SDW are still present [27]. The low energy electronic structure ultimately determines the resistivity of the material. We have measured the resistance of a doped sample from the same batch as was used for ARPES [Fig. 4(a)]. Above the superconducting drop at $T_c = 32$ K a linear regime is found which evolves into a smooth curve around $T \approx 150$ K [Fig. 4(a)] before saturating in linear behavior again at $T \approx 300$ K. This is best seen in the temperature derivative in Fig. 4(b). The result is very similar to other pnictide families [27] and to previously published data on $Ba_{1-x}K_xFe_2As_2$ [28]. The inset of Fig. 4(a) shows the temperature dependence of the Fermi velocity obtained from the dispersions in Fig. 2(a) by fitting the low energy region ($E = 0 \ldots 20$ meV) to a line. (Note that the value for the ΓX direction at low T but above T_c is also close to 0.5 eV Å.) It is clear that v_F changes substantially when the slope of ρ starts to change. Generally, a relation between the Fermi velocity and conductivity is to be expected. According to the semiclassical Boltzman equation for a tetragonal two-dimensional system it holds

$$\rho(T) \sim \left(\int_{FS} v_F(\mathbf{k}, T) \tau(\mathbf{k}, T) dk \right)^{-1},$$

where τ is the lifetime and the integration runs over Fermi surface segments dk. By setting $v_F(\mathbf{k}) = \text{const}$, $\tau^{-1} \sim T$ [which is suggested by the linear dependence of $R(T)$

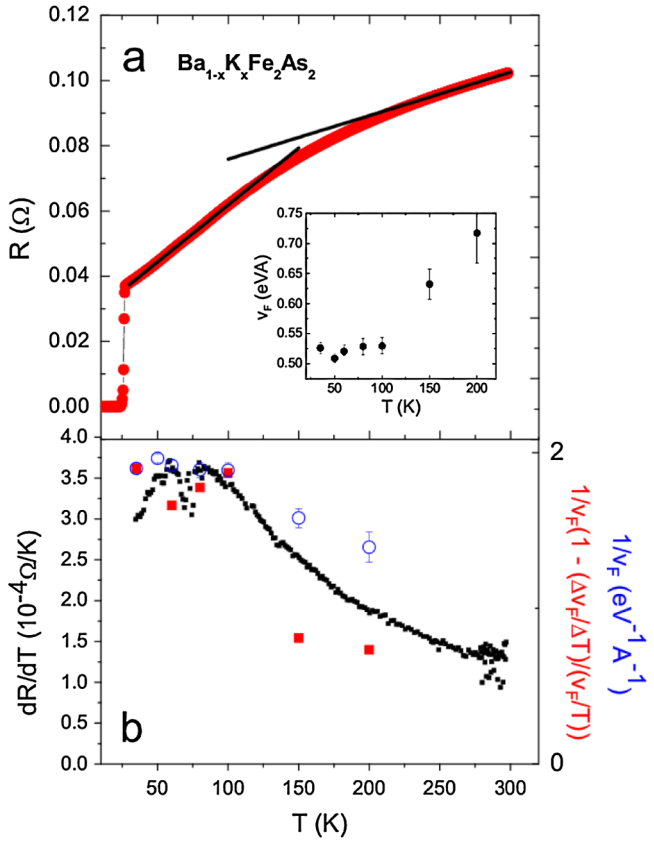

FIG. 4 (color online). (a) Resistance of $Ba_{1-x}K_xFe_2As_2$. Black lines are guides to the eye. Inset: Fermi velocities extracted from data in Fig. 2(a). (b) Temperature derivative of the resistance compared to functions of v_F.

below ~100 K, i.e., in a region where $v_F(T) \approx$ const] and restrict the integral to the inner, concentric Γ-FS (which inherently assumes that the other FS's mirror its behavior), we obtain the scaling relation

$$\frac{d\rho}{dT} \sim \frac{1}{v_F}\left(1 - \frac{dv_F/dT}{v_F/T}\right).$$

Figure 4(b) shows qualitative agreement between ARPES and resistivity data based on this rough estimate which suggests that the same fluctuations that determine the shape of the resistivity curve are responsible for the kink renormalization.

Recent results from μSR point to a pronounced phase separation for doped $Ba_{1-x}K_xFe_2As_2$ and $Sr_{1-x}Na_xFe_2As_2$ [29,30] into regions with *static* magnetic order and superconducting/paramagnetic volume fraction. Hence there might be an intrinsic mixture of coupling strength for ARPES experiments. To elucidate the role of these inhomogeneities careful doping-dependent studies are necessary.

In conclusion, we have investigated the low energy electronic structure of $Ba_{1-x}K_xFe_2As_2$ ($x = 0$; 0.3) by angle-resolved photoemission spectroscopy. We find a kink-like low energy renormalization of the dispersion, situated at $E = 25$ meV for $x = 0.3$ and $E = 45$ meV for $x = 0$. The kink in the doped compound is found for both high symmetry directions ΓX and ΓM. The kink is temperature insensitive below $T = 100$ K but vanishes at $T = 200$ K for the doped compound. In particular the kink does not change across T_c ruling out the magnetic resonance mode as its origin. Using a simple model we find that the temperature dependence of the Fermi velocity mirrors that of the resistivity. The experimental findings render conventional electron-phonon coupling as origin of the kink unlikely and imply either the presence of an exotic electron-phonon coupling mechanism, or the relevance of another coupling channel for the charge carriers which is naturally associated to magnetic fluctuations, both in the normal and in the superconducting state.

We acknowledge financial support by the DFG (KN 393/12-1). We thank H. Eschrig for stimulating discussions.

[1] Y. Kamihara *et al.*, J. Am. Chem. Soc. **130**, 3296 (2008).
[2] C. Wang *et al.*, Europhys. Lett. **83**, 67 006 (2008).
[3] C. Liu *et al.*, arXiv:0806.2147.
[4] H. Ding *et al.*, Europhys. Lett. **83**, 47 001 (2008).
[5] D. V. Evtushynsky *et al.*, Phys. Rev. B **79**, 054517 (2009).
[6] L. Zhao *et al.*, Chin. Phys. Lett. **25**, 4402 (2008).
[7] L. X. Yang et al., Phys. Rev. Lett. **102**, 107002 (2009).
[8] L. Boeri *et al.*, Phys. Rev. Lett. **101**, 026403 (2008).
[9] C. de la Cruz *et al.*, Nature (London) **453**, 899 (2008).
[10] H.-H. Klauss *et al.*, Phys. Rev. Lett. **101**, 077005 (2008).
[11] A. D. Christianson *et al.*, Nature (London) **456**, 930 (2008).
[12] M. M. Korshunov and I. Eremin, Phys. Rev. B **78**, 140509 (R) (2008).
[13] A. Damascelli *et al.*, Rev. Mod. Phys. **75**, 473 (2003).
[14] P. Richard *et al.*, Phys. Rev. Lett. **102**, 047003 (2009).
[15] L. Wray *et al.*, Phys. Rev. B **78**, 184508 (2008).
[16] G. L. Sun, D. L. Sun, and C. T. Lin, arXiv:0901.2728.
[17] V. B. Zabolotnyy *et al.*, Nature (London) **457**, 569 (2009).
[18] A. A. Kordyuk *et al.*, Phys. Rev. B **71**, 214513 (2005).
[19] A. D. Christianson *et al.*, Phys. Rev. Lett. **101**, 157004 (2008).
[20] A. P. Litvinchuk *et al.*, Phys. Rev. B **78**, 060503(R) (2008).
[21] S. C. Zhao *et al.*, Supercond. Sci. Technol. **22**, 015017 (2009).
[22] Y. Gallais *et al.*, Phys. Rev. B **78**, 132509 (2008).
[23] H. Eschrig, arXiv:0804.0186.
[24] M. Le Tacon *et al.*, Phys. Rev. B **78**, 140505(R) (2008).
[25] K.-Y. Choi *et al.*, Phys. Rev. B **78**, 212503 (2008).
[26] R. A. Ewings *et al.*, Phys. Rev. B **78**, 220501 (2008).
[27] C. Hess *et al.*, arXiv:0811.1601.
[28] M. Rotter *et al.*, arXiv:0812.2827.
[29] T. Goko *et al.*, arXiv:0808.1425.
[30] J. T. Park *et al.*, Phys. Rev. Lett. **102**, 117006 (2009).